Available online at www.sciencedirect.com

SciVerse ScienceDirect

Journal of Nutritional Biochemistry 23 (2012) 320–331

Journal of Nutritional Biochemistry

RESEARCH ARTICLES

Purple corn anthocyanins dampened high-glucose-induced mesangial fibrosis and inflammation: possible renoprotective role in diabetic nephropathy☆,☆☆

Jing Li[a], Soon Sung Lim[a], Jae-Yong Lee[b], Jin-Kyu Kim[c], Sang-Wook Kang[a], Jung-Lye Kim[a], Young-Hee Kang[a,c,*]

[a]Department of Food and Nutrition and the Regional Research Universities Program/Medical & Bio-Materials Research Center, Hallym University, Chuncheon 200-702, Korea
[b]Department of Biochemistry, College of Medicine, Hallym University, Chuncheon 200-702, Korea
[c]Institute of Natural Medicine, Hallym University, Chuncheon 200-702, Korea

Received 14 July 2010; received in revised form 29 November 2010; accepted 9 December 2010

Abstract

Purple corn has been classified as a functional food rich in anthocyanins possessing potential disease-preventive properties. This study examined whether purple corn anthocyanins (PCA) mainly comprised cyanidin 3-glucoside and cyanidin-3-(6″-malonylglucoside) can attenuate high-glucose (HG)-promoted mesangial cell (MC) proliferation and matrix accumulation, major features of diabetic glomerulosclerosis. Human renal MC were cultured for 3 days in media containing 5.5 mM glucose plus 27.5 mM mannitol as osmotic controls or media containing 33 mM glucose in the absence and presence of 1–20 μg/ml PCA. The HG exposure of MC caused substantial increases in connective tissue growth factor (CTGF) expression and collagen IV secretion with mesangial hyperplasia, which were repealed by adding PCA. PCA boosted HG-plummeted membrane type-1 matrix metalloproteinase expression and dampened HG-elevated tissue inhibitor of matrix metalloproteinase-2 expression through disturbing transforming growth factor β (TGF-β)–SMAD signaling, facilitating extracellular matrix degradation. This study further revealed that PCA ameliorated HG-inflamed mesangial inflammation accompanying induction of intracellular cell adhesion molecule-1 and monocyte chemoattractant protein-1 (MCP-1) responsible for CTGF expression. The induction of intracellular cell adhesion molecule-1 and MCP-1 was mediated via TGF-β signaling, which was suppressed by PCA. In addition, the HG-promoted CTGF expression entailed nuclear factor κB (NF-κB) signaling involved in MCP-1 transcription. The HG–TGF-β induction was blocked in the presence of a NF-κB inhibitor, and the nuclear NF-κB translocation was blunted by a TGF-β receptor 1 inhibitor. PCA dampened NF-κB translocation in HG-exposed MC. These results demonstrate that there was a crosstalk between TGF-β–SMAD and NF-κB pathways in the diabetes-associated mesangial fibrosis and inflammation, which appeared to be severed by PCA.

Keywords: High glucose; Purple corn anthocyanins; Mesangial inflammation; Renal fibrosis

1. Introduction

Diabetic nephropathy (DN) is characterized by aberrant alterations such as extracellular matrix (ECM) accumulation ultimately leading to chronic renal failure [1]. The first and most distinctive glomerular lesion of diabetes is mesangial expansion concurrently accompanying mesangial hyperplasia, which precedes interstitial disease called diabetic glomerulosclerosis [2,3]. A boosted production of matrix-synthesizing growth factors and a diminished formation of matrix-degrading proteases can be responsible for hyperglycemia-associated accumulation of ECM constituents at the glomerular levels [4,5]. Connective tissue growth factor (CTGF) is thought to express in the mesangium and play an important role in the ECM-synthesizing process [1,4,6]. In contrast, the enzymatic breakdown of ECM requires matrix metalloproteinases (MMP) as key matrix-degrading proteases [5,7]. Hyperglycemia triggers intracellular signaling pathways to stimulate induction of fibrogenic and prosclerotic cytokines activating ECM deposition [3,8].

Increased transforming growth factor β (TGF-β) is thought to be the key fibrogenic cytokine involved in the progression of DN [9]. It was shown that high ambient glucose presumed as an instigating

Abbreviations: CTGF, connective tissue growth factor; DMEM, Dulbecco's modified Eagle's media; DN, diabetic nephropathy; ECM, extracellular matrix; FBS, fetal bovine serum; HG, high glucose; HRMC, human renal mesangial cells; ICAM-1, intracellular cell adhesion molecule-1; MCP-1, monocyte chemoattractant protein-1; MMP, matrix metalloproteinases; MT1-MMP, membrane type-1 matrix metalloproteinase; MTT, 3-(4,5-dimetylthiazol-yl)-diphenyl tetrazolium bromide; PBS-T, phosphate-buffered saline–Tween 20; PCA, purple corn anthocyanins; ROS, reactive oxygen species; RT-PCR, reverse transcriptase-polymerase chain reaction; TGF, transforming growth factor; TGF-βR1, transforming growth factor-β receptor kinase 1; TIMP, tissue inhibitors of matrix metalloproteinases.

☆ Sources of funding: This study was supported by the grant from the Ministry for Food, Agriculture, Forestry and Fisheries through Korea Institute of Planning and Evaluation for Technology of Food, Agriculture, Forestry and Fisheries (109163-03-1-SB030) and by the grant from the National Research Foundation of Korea (2009-0072534).

☆☆ Author disclosures: J. Li, S.S. Lim, J.Y. Lee, J.K. Kim, S.W. Kang, J.L. Kim and Y.H. Kang have no conflict of interest.

* Corresponding author. Department of Food and Nutrition, Hallym University, Chuncheon, Kangwon-do, 200-702, South Korea. Tel.: +82 33 248 2132; fax: +82 33 254 1475.

E-mail address: yhkang@hallym.ac.kr (Y.-H. Kang).

0955-2863/$ - see front matter © 2012 Elsevier Inc. All rights reserved.
doi:10.1016/j.jnutbio.2010.12.008

agent-enhancing ECM accumulation stimulated resident renal cells to produce TGF-β1 [9,10]. There is accumulating evidence demonstrating that the diabetes-associated nephropathy is closely related to mesangial inflammation [11,12]. In diabetic patients with nephropathy, the levels of certain proinflammatory factors such as intercellular cell adhesion molecule-1 (ICAM)-1 and monocyte chemoattractant protein-1 (MCP-1) were elevated [11]. ICAM-1 appeared to recruit inflammatory immune cells such as macrophages and granulocytes [11,12]. MCP-1, a potent chemokine involved in the recruitment of macrophages, appeared to be responsible for diabetic ECM accumulation and early inflammation in diabetic kidney diseases [13]. However, the crosstalk between mesangial fibrosis and inflammation has not yet been well defined.

Numerous studies demonstrated that natural compounds diminished renal stress-triggered inflammation [14,15]. Isoflavone puerarin suppressed mesangial inflammation induced by advanced glycation end products likely through the induction of heme oxygenase-1 expression [15]. In addition, the natural product colchicine dampened inflammatory cell infiltration and ECM accumulation in DN, which entailed blockade of ICAM-1 and MCP-1 expression [16]. It is deemed that these natural compounds may retard mesangial inflammation and ECM accumulation via disturbing inflammatory and fibrogenic pathways. Accordingly, the renoprotection of natural compounds against mesangial inflammation may be specific therapies of renal fibrosis in DN.

Purple corn, known as *Zea mays* L., has been cultivated in South America, mainly in Peru and Bolivia, and used for centuries as a natural food colorant and drinks. Purple corn extract is shown to be rich in anthocyanins and functional phenolics [17]. Anthocyanins have been reported to exhibit antiangiogenic, antidiabetic and anticarcinogenic properties [18–20]. Dietary purple corn color inhibited 7,12-dimethylbenz[*a*]anthracene-induced mammary carcinogenesis, in which cyanidin 3-glucoside, a major anthocyanin present in purple corn color, acted as a chemopreventive and chemotherapeutic agent [21]. In addition, anthocyanin-rich purple corn extract suppressed proliferation of human colorectal adenocarcinoma HT29 cells and exerted an additive interaction with the other phenolics [22].

Based on possible antidiabetic virtues of purple corn extract, this study attempted to determine whether purple corn anthocyanins (PCA) may prevent high-glucose (HG)-induced glomerulosclerosis and renal fibrosis. The alteration of collagen IV accumulation was investigated by treating PCA to HG-exposed human renal mesangial

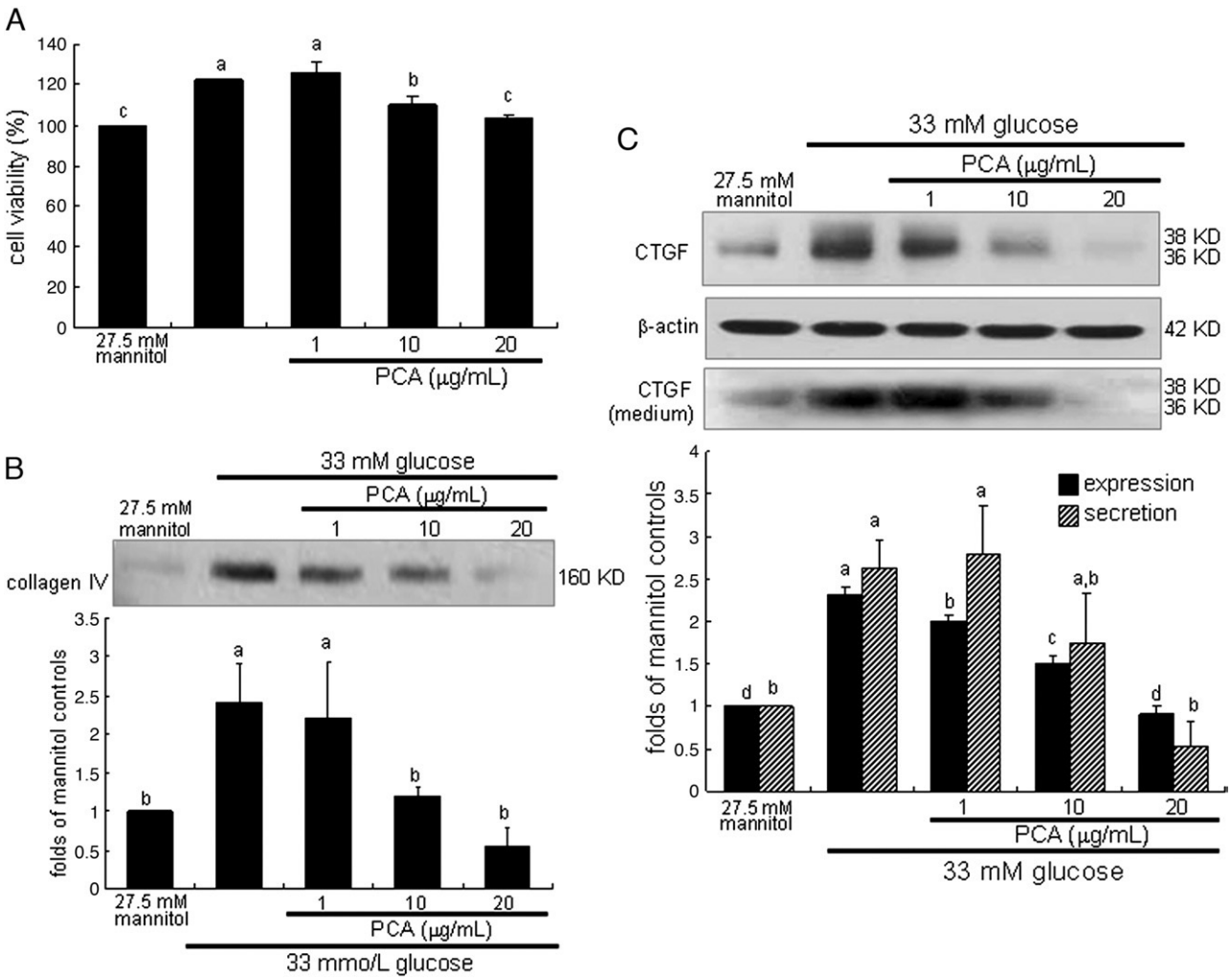

Fig. 1. Inhibition of HG–mesangial cell proliferation (A), collagen IV secretion (B) and CTGF production (C) by PCA. HRMCs were challenged with 5.5 mM glucose plus 27.5 mM mannitol as osmotic controls or with 33 mM glucose in the absence and presence of 1–20 μg/ml PCA. Values of cell viability and proliferation are mean±S.E.M. (n=5) and expressed as percent cell survival relative to 27.5 mM mannitol controls (cell viability=100%). Collagen IV secretion and CTGF production were measured by using Western blot analyses with cell lysates or culture media. Representative blots shown are typical of three independent experiments. The bar graphs (mean±S.E.M., n=3) in the bottom panel represent quantitative results obtained from a densitometer. Values not sharing a letter are significantly different at P<.05.

cells (HRMCs). Expression of CTGF and membrane type-1 MMP (MT-1 MMP) was assessed to define a cardinal role of PCA in inhibiting ECM amassing in DN. This study elucidated a potential role of TGF-β–SMAD signaling in the matrix remodeling leading to renal fibrosis. Furthermore, it was explored that the diabetes-associated mesangial matrix remodeling may be linked to inflammation instigated by ICAM-1 and MCP-1 and that PCA can interfere with possible crosstalk between mesangial fibrosis and inflammation through nuclear factor (NF)-κB-dependent mechanisms.

2. Materials and methods

2.1. Chemicals

Fetal bovine serum (FBS), trypsin–EDTA and penicillin–streptomycin were obtained from BioWhittaker (San Diego, CA, USA). 3-(4, 5-Dimetylthiazol-yl)-diphenyl tetrazolium bromide (MTT) was purchased from DUCHEFA Biochemie (Haarlem, the Netherlands). Dulbecco's modified Eagle's media (DMEM), Nutrient Mixture F-12 Ham medium, mannitol, D-glucose and human recombinant MCP-1 were supplied by Sigma Chemical (St. Louis, MO, USA), as were all other reagents, unless specifically stated otherwise. Antibody of human CTGF was obtained from AbCam (Cambridge, UK), and antibodies of human collagen IV, MT1-MMP, ICAM-1 and NF-κB were provided by Santa Cruz Biotechnology (Santa Cruz, CA, USA). Human tissue inhibitor of MMP-2 (TIMP-2) and SMAD7 antibody, and human recombinant proteins of TGF-β1 were provided by R&D systems (Minneapolis, MN, USA). Antibodies of human TGF-β1, SMAD4, phospho-SMAD2 and total-SMAD2 were obtained from Cell Signaling Technology (Beverly, CA, USA). The NF-κB inhibitor SN50 was bought from Biomol-Enzo Life Sciences (Plymouth, PA, USA). Horseradish peroxidase-conjugated goat antirabbit immunoglobulin G (IgG), goat antimouse and donkey antigoat IgG were obtained from Jackson ImmunoResearch Laboratories (West Grove, PA, USA). Powder of purple corn kernels was provided by Brilliant Project International (Seoul, Korea).

Table 1
Identification of the major anthocyanins detected in the kernel of purple corn

Peaks	R_t (min)	UV/Vis λ_{Max} (nm)	LC-ESI-MS		Compounds[a]
			$[M]^+$ (m/z)	Fragments $[M+H]^+$ (m/z)	
1	7.45	515, 279	449	287	cy3-G
2	10.47	504, 278	433	271	pg3-G
3	12.98	515, 279	463	301	pn3-G
4	18.47	517, 280	535	449,287	cy3-(6-mal-G)
5	21.73	504, 350, 264	519	271	pg3-(6-mal-G)
6	22.02	525, 279	621	287	cy3-(dimal-G)
7	23.38	517, 279	549	301	pn3-(6-mal-G)
8	24.13	525, 279	491	287	cy3-(6-acet-G)

[a] Compounds 1–8 (shown in Fig. 2A) were identified based on photodiode-array absorbance and mass fragmentation pattern. R_t, retention time; UV/Vis, ultraviolet–visible spectroscopy; LC-ESI-MS, liquid chromatography–electrospray ionization–mass spectrometry; $[M]^+$, molecular ion; $[M+H]^+$, protonated precursor ion; m/z value, mass-to-charge ratio. A mass spectrum is intensity versus m/z plot representing a chemical analysis.

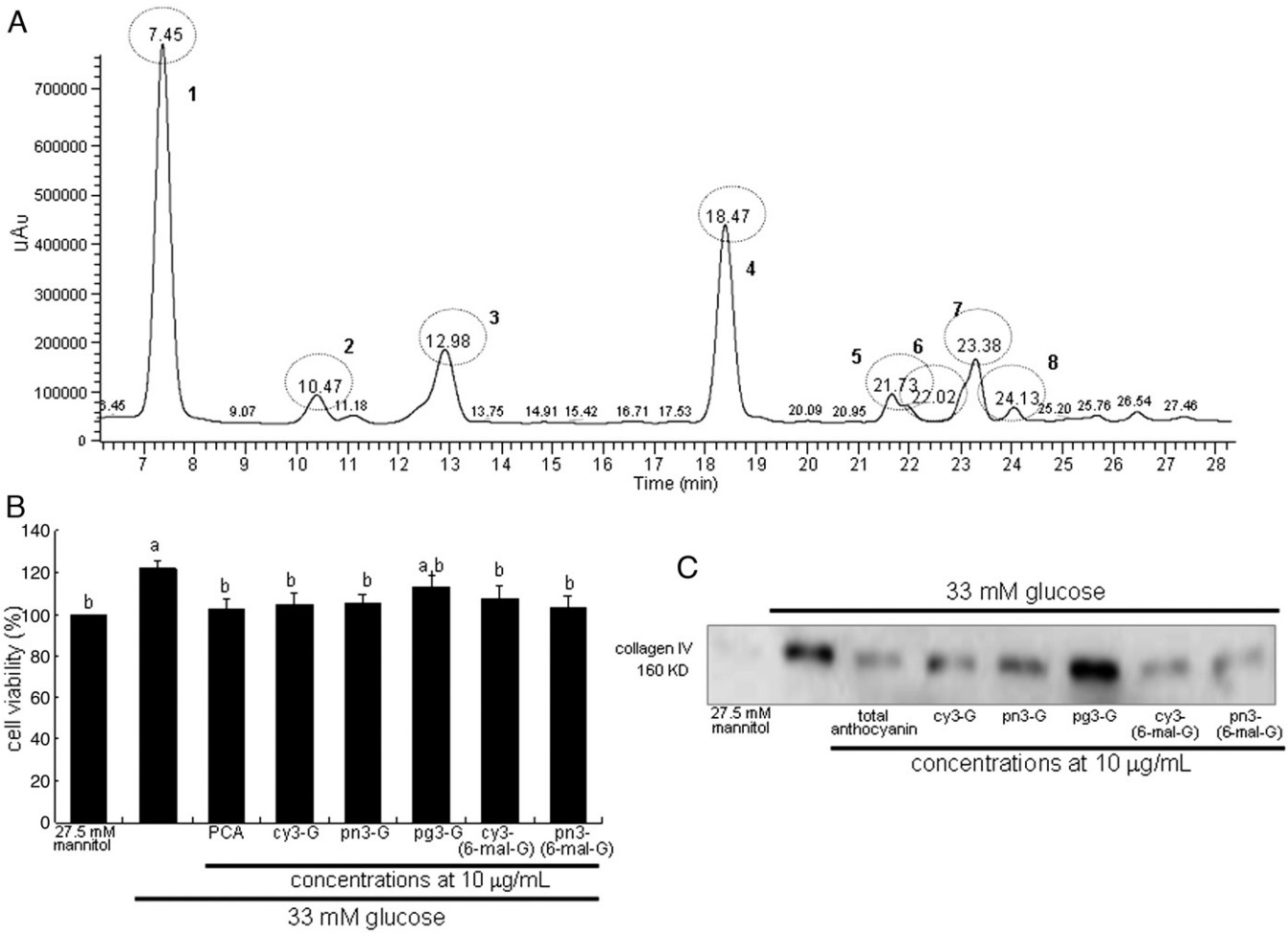

Fig. 2. HPLC spectra at l=570 nm showing major anthocyanins detected in the kernel extract of purple corn (A), and their effects on HRMCs (HRMC) viability (B) and collagen IV secretion (C). HRMC were exposed to 5.5 mM glucose plus 27.5 mM mannitol as osmotic controls or with 33 mM glucose in the absence and presence of 10 μg/ml PCA and 10 μg/ml of each anthocyanin isolated from purple corn extract. Values of cell viability and proliferation are mean±S.E.M. (n=5) and expressed as percent cell survival relative to 27.5 mM mannitol controls (cell viability=100%). Values not sharing a letter are significantly different at P<.05. Collagen IV secretion in culture media was measured by using Western blot analyses. Representative blots shown are typical of three independent experiments.

2.2. Mesangial cell culture and proliferation

HRMCs (Sciencell Research Laboratories, Carlsbad, CA, USA) were cultured at 37°C humidified atmosphere of 5% CO_2 in air. Routine culture of HRMC was performed in DMEM plus F12 (7:1) media containing 15% FBS, 2 mM glutamine, 100 U/ml penicillin, 100 μg/ml streptomycin. HRMC in passage of 6–10 were subcultured at 80% confluence and used for further experiments. To mimic diabetic renal fibrosis caused by chronic hyperglycemia, HRMCs were incubated in 33 mM glucose-added DMEM containing 2% FBS and 8 μg/ml insulin for 3 days in the absence and presence of PCA. For osmotic control incubations, another set of HRMC was cultured in DMEM containing 2% FBS (+2 μg/ml insulin) and supplemented with 27.5 mM mannitol. PCA was supplemented at concentrations of 1−25 μg/ml for 3-day culture experiments.

After the 3-day incubation period, the MTT assay was performed for measuring cell proliferation [23]. HRMCs were incubated in a fresh phenol red-free DMEM containing 1 g/l MTT for 3 h at 37°C. After unconverted MTT was removed, the purple formazan product was dissolved in isopropanol with gentle shaking. Absorbance of formazan dye was measured at λ=570 nm, with background subtraction using λ=690 nm.

2.3. Western blot analysis

Western blot analysis was conducted using whole cell lysates and collected culture media prepared from HRMC at a density of 3.0×10^5 cells [24]. Whole mesangial cell lysates were prepared in a lysis buffer containing 1 M β-glycerophosphate, 1% β-mercaptoethanol, 0.5 M NaF, 0.1 M Na_3VO_4 and protease inhibitor cocktail. Cell lysates containing equal amounts of total proteins or equal volumes of culture medium were electrophoresed on 6%–10% sodium dodecyl sulfate polyacrylamide gel electrophoresis (SDS-PAGE) and transferred onto a nitrocellulose membrane. Nonspecific binding was blocked by soaking the membrane in a TBS-T buffer [50 mM Tris-HCl (pH 7.5), 150 mM NaCl and 0.1% Tween 20] supplemented with 3% bovine serum albumin for 3 h. The membrane was incubated with an antibody to human proteins of CTGF, collagen IV, MT1-MMP, TIMP-2, TGF-β, SMAD4, phospho-SMAD2, SMAD2, SMAD7, ICAM-1 and NF-κB. Subsequently, the membrane was then incubated with a secondary antibody of goat antirabbit IgG, goat antimouse IgG or donkey antigoat IgG conjugated to horseradish peroxidase. Each protein level was determined by using Supersignal West Pico Chemiluminescence detection reagents (Pierce Biotechnology, Rockford, IL, USA) and Konica X-ray film (Konica Co., Tokyo, Japan). Incubation with mouse antihuman β-actin antibody was conducted for the comparative control.

2.4. PCA extraction and high-performance liquid chromatography/mass spectrometry analyses

Powder of purple corn kernels was extracted with ethanol for 12 h at 25°C. The extract obtained was decanted and filtered to give a crude extract. The extracted solution was evaporated under reduced pressure to dryness, and dryness residue was applied to a glass open column (10×300 mm I.D.) packed with Diaion HP-20 (Mitsubishi Kasei Co., Tokyo, Japan) and eluted with water for washing of sugar or the impure components, followed by ethanol for anthocyanin-rich fractions. Separation of anthocyanins was conducted on a reverse-phase Capcell Pak C18 UG 120 S5 column (4.6×150 mm I.D., 4 μm; Shiseido Co., Ltd, Tokyo, Japan) using a Finnigan Surveyor high-performance liquid chromatography (HPLC) system (Thermo Quest, San Jose, CA, USA) at ambient temperature. The mobile phase was a binary elution of 5% formic acid solution (A) and 100% methanol (B) under the following gradient conditions: initial, 20% B; 7 min, 20% B; 15 min, 25% B; 32 min, 50% B; 36 min, 100% B; 38 min, 100% B; 40 min, 20% B and 45 min, 20% B. The flow rate was 700 μl/min, and the injection volume was 10 μl. Eluted substances were detected at 520 nm with a photodiode-array detector between 200 and 600 nm with a bandwidth of 1 nm.

For the identification of major anthocyanins, the column elute was split, and 0.2 $ml\cdot min^{-1}$ was directed to a Finnigan LCQ Advantage ion-trap MS (Thermo Quest)

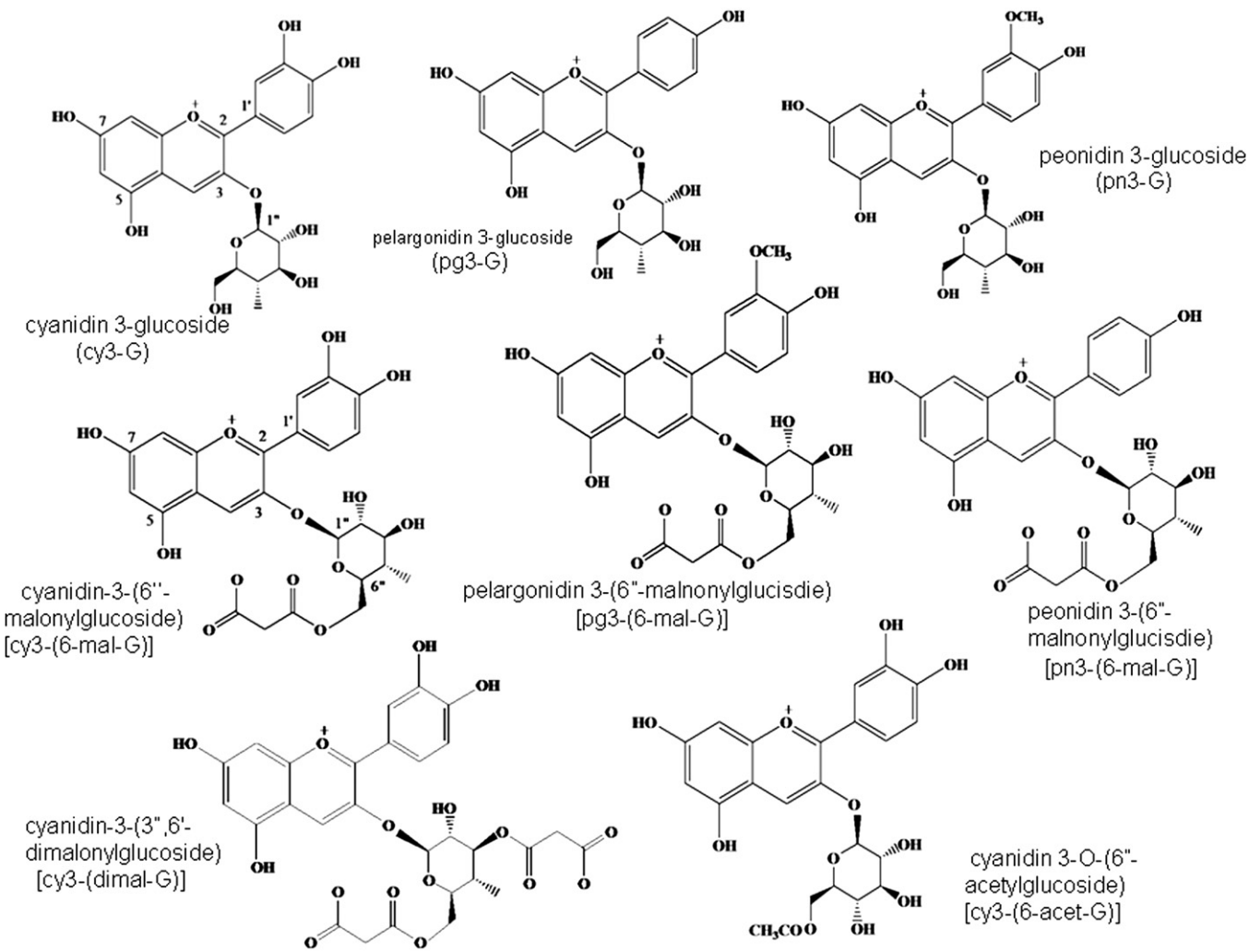

Fig. 3. Chemical structures of anthocyanins identified in the kernel of purple corn. The retention time and HPLC spectrum of major anthocyanins detected in purple corn kernels were shown in Fig. 2 and Table 1.

equipped with an electrospray ionization (ESI) interface after passing through the flow cell of the photodiode-array detector. Analysis was carried out using the positive ion monitoring at a capillary temperature of 280°C, spray voltage of 5.5 kV, capillary voltage of 10 V and tube lens offset of −5.0 V. Spectral data were recorded with He gas as a collision gas. Anthocyanins were detected using *m/z* value following MS/MS. The MS/MS collision energy was set to 35%. Data were collected using dual analysis in full-scan mode from 100 to 1000 atomic mass units and MS/MS modes. Data were processed using the Xcalibur 2.0 version software program (Thermo Electron Corporation, San Jose, CA, USA).

2.5. Gelatin zymography

After HG culture for 3 days under starved condition, culture media were collected and gelatin zymography for MMP-2 was performed [25]. Culture media were electrophoresed on 8% SDS-PAGE (0.3 mM Tris-HCl, pH 6.8, 4% SDS, 20% glycerol and 0.03% bromophenol blue) copolymerized with 0.1% gelatin as the substrate. The gel was incubated for 1 h in 2.5% Triton X-100 solution, followed by incubation for 20 h in 50 mM Tris-HCl buffer (pH 7.5), containing 0.05% Brij-35. The gels were stained with 0.1% Coomassie brilliant blue G-250 and 2% acetic acid.

2.6. Transcriptional reporter gene assay

To evaluate the promotor activity of the ICAM-1, a promoter–reporter construct with pGL3-basic vector with luciferase gene driven by the translucent ICAM-1-promoter (Cosmo Co., Seoul, Korea) was introduced. A pGL3-basic vector reporter construct was used as a transfectional control. Nucleofection in HRMC with an ICAM-1 reporter construct was conducted for the gene delivery according to the optimized transfection protocols supplied by the manufacturer (Amaxa Biosystem, Cologne, Germany). Briefly, HRMCs were suspended in an Amaxa cuvette with 100 μl nucleofector solution, mixed with 3 μg ICAM-1 reporter vector and pulsed in the nucleofector device (program A-33). Cells were immediately transferred into prewarmed fresh medium in 6-well plates. After 24-h nucleofection, transfected cells were starved for 24 h and exposed to HG media containing 10 μg/ml PCA for 3 days. After washing the cells, 100 μl of cell lysis reagent was added. Promoter activity of HRMC nucleofected with a luciferase-harboring ICAM-1 promoter construct was determined using the dual-luciferase reporter kit (Promega Biosciences). For the measurement of luciferase activity, 20 μl of lysate mixed with 100 μl of assay reagent was assayed using a luminometer (Lumat LB 9501, Berthold, Germany).

2.7. Analyses of reverse transcriptase-polymerase chain reaction and real-time polymerase chain reaction

Following HG-PCA culture protocols, total RNA was isolated from 6×10^5 HRMC using a commercially available Trizol reagent kit (Invitrogen, Carlsbad, CA, USA). Isolated RNA (5 μg) was reversibly transcribed with 200 units of reverse transcriptase and 0.5 g/l oligo-$(dT)^{15}$ primer (Bioneer, Korea). The expression of messenger RNA (mRNA) transcripts of human MCP-1 (forward primer: 5′-AACTGAAGCTCGCACTCTCG-3′, reverse primer: 5′-TCAGCACAGATCTCCTTGGC-3′, 258 bp) and β-actin (forward primer: 5′-GACTACCT-CATGAAGATC-3′, reverse primer: 5′-GATCCACATCTGCTGGAA-3′, 500 bp) were determined by reverse transcriptase-polymerase chain reaction (RT-PCR). The PCR assay was conducted in 25 μl of 10 mM Tris-HCl (pH 9.0) containing 25 mM $MgCl_2$, 10 mM dNTP, 5 units of Taq DNA polymerase and 10 μM of each primer and began with 5-min denaturation at 94°C followed by 30 PCR cycles [24]. Each cycle consisted of 60 s at 94°C, 60 s at 55°C and 60 s at 72°C, and the final extension was for 10 min at 72°C. After themocycling, 15 μl of PCR products was electrophoresed on 1% agarose-formaldehyde gel containing 0.5 m g/l ethidium bromide. The bands were visualized using a TFX-20M model-UV transilluminator (Vilber-Lourmat, France), and gel photographs were taken. The contaminant-free condition was routinely checked by the RT-PCR assay with negative control samples without a primer addition.

Real-time RT-PCR also quantified the levels of mRNA transcripts of MCP-1 (forward primer: 5′-GATCTCAGTGCAGAGGCTCG-3′, reverse primer: 5′-TGCTTGTCCAGGTGGTC-CAT-3′, 153 bp) and glyceraldehyde-3-phosphate dehydrogenase (forward primer: 5′-GAAGGTGAAGGTCGGAGTC-3′, reverse primer: 5′-GAAGATGGTGATGGGATTTC-3′) using SYBR Green PCR kit (Qiagen, Valencia, CA, USA). Data analysis of real-time PCR results and calculation of the relative quantification were performed using the Delta CT analysis by the Rotor-gene software version 6.0 (Corbett Research, Australia). The housekeeping gene glyceraldehyde-3-phosphate dehydrogenase was used for internal normalization. The standard PCR conditions were 94°C for 10 min, then 40 cycles at 94°C (30 s), 60°C (30 s) and 72°C (60 s), followed by the melting curve analysis.

2.8. Immunocytochemistry

After HRMCs grown on 24-well glass slides were rinsed with phosphate-buffered saline containing 0.2% Tween 20 (PBS-T), cells were fixed with 4% ice-cold formaldehyde for 20 min and permeated with 0.1% Triton X-100 and 0.1% sodium citrate for 2 min on ice [24]. After washing, fixed cells were incubated with human NF-κB p65 antibody in PBS-T at 4°C overnight. Cells were incubated with fluorescein isothiocyanate-conjugated antirabbit IgG in PBS-T as a secondary antibody. Fluorescent microphotography images were obtained by an Axiomager Optical fluorescence microscope (Zeiss, Germany).

2.9. Nuclear extract preparation

Cytosolic and nuclear protein fractions were prepared by a detergent lysis procedure to determine the translocation of NF-κB. The cells were lysed in 10 mM HEPES buffer (pH 7.9, 10 mM KCl, 0.4 mM phenylmethylsulfonyl fluoride, 1 mM dithiothreitol, 1 mM EDTA, 0.5% Nonidet P40, 20 mg/l of each of aprotinin, antipain and leupeptin) and incubated on ice for 1 h. Nuclei were pelleted by a centrifugation at 3000×*g* for 20 min. Proteins were extracted from nuclear pellets by incubation in a high-salt buffer containing 420 mM NaCl, 20 mM HEPES [(pH 7.9), 0.4 mM phenylmethylsulfonyl fluoride, 1 mM dithiothreitol, 1 mM EDTA, 20% glycerol and 10 μg/ml of each of aprotinin, antipain and leupeptin] at 4°C with vigorous shaking. The nuclear debris was pelleted by a brief centrifugation at 20,000×*g* for 30 min, and the supernatant was stored for further experiments.

2.10. Data analysis

Data were presented as mean±S.E.M. Statistical analyses were performed using Statistical Analysis Systems statistical software package (SAS Institute Inc., Cary, NC, USA). Significance was determined by one-way analysis of variance, followed by Duncan range test for multiple comparisons. Differences were considered significant at $P<.05$.

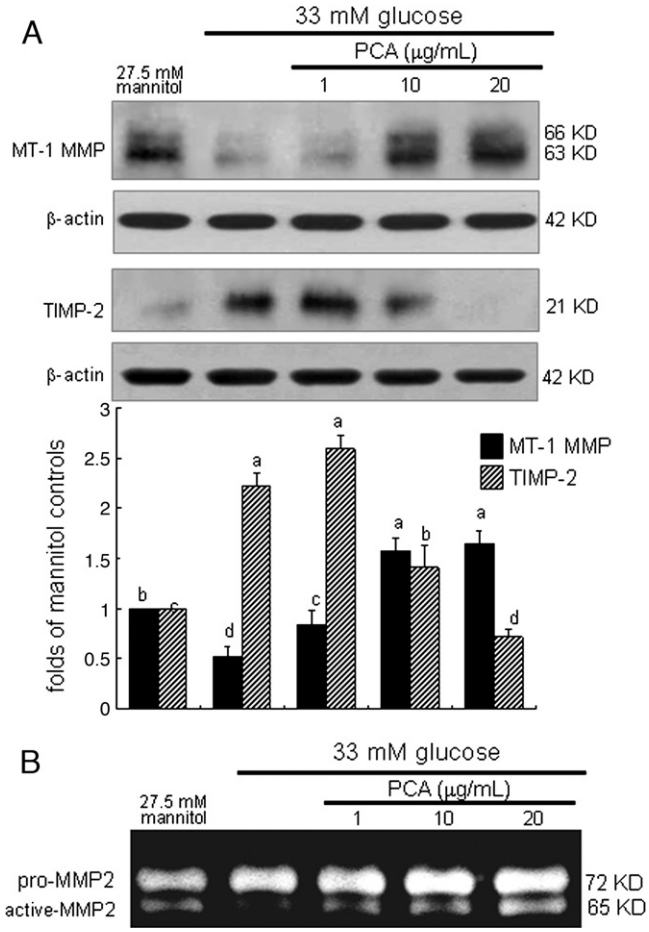

Fig. 4. Western blot data (A) showing expression of MT-1 MMP and TIMP-2, and zymography showing MMP-2 activity (B) in HRMCs treated with PCA under HG conditions. Cells were supplemented with 1–20 μg/ml PCA and then exposed to 33 mM glucose for 3 days. In addition, HRMCs were incubated for 3 days in 5.5 mM glucose and 27.5 mM mannitol as osmotic controls. After HRMC culture protocols, Western blot analysis was conducted with cell lysates and with a primary antibody against MT-1 MMP and TIMP-2. β-Actin protein was used as an internal control. The bar graphs (mean±S.E.M., $n=3$) in the bottom panel represent quantitative results obtained from a densitometer. Values not sharing a letter are significantly different at $P<.05$. For gelatin zymography measuring MMP-2 activity (B), collected culture media were run for electrophoresis on 8% SDS-PAGE copolymerized with 0.1% gelatin as the substrate (three separate experiments).

3. Results

3.1. Effect of PCA on HG-induced mesangial hyperplasia and fibrosis

This study evaluated whether HG stimulated mesangial cell proliferation and whether PCA reversed it. HG caused HRMC proliferation with ≈20% increase in cell viability, measured by MTT assay. In contrast, ≥10 μg/ml PCA dose-dependently inhibited such proliferative activity of ambient HG without any cytotoxicity (Fig. 1A). It is deemed that PCA ameliorated mesangial hyperplasia in the DN pathogenesis.

Mesangial matrix accumulation was shown to be responsible for renal fibrosis [4,24]. To investigate inhibitory effects of PCA on HG-instigated mesangial matrix expansion, production of collagen IV and CTGF was examined. HG-elevated fibrogenic collagen IV secretion, which was attenuated by adding ≥10 μg/ml PCA (Fig. 1B). In addition, HG-augmented production of CTGF was suppressed in PCA-treated HRMC (Fig. 1C). Collagen IV secretion encumbered by PCA was most likely attributed to decreased CTGF production due to its supplementation.

3.2. Identification of individual anthocyanins in PCA

The extract of purple corn kernel was evaluated for quantitative and qualitative composition of anthocyanins as well as total phenolics. High variability was observed on contents of monomeric anthocyanins and phenolics with yields ranging from 290 to 1333 mg/100 g dry weight^{-1} and from 950 to 3516 mg/100 g dry weight^{-1}, respectively, while 30.5%–47.1% of total phenolics were anthocyanins (data not shown). In addition, 35.6%–54.0% of the anthocyanins were acylated.

HPLC spectra at λ=570 nm showed that eight anthocyanins were distinctly detected with different retention times (Fig. 2A). The eight major anthocyanins were identified as cyanidin-3-glucoside (cy3-G), pelargonidin-3-glucoside (pg3-G), peonidin-3-glucoside (pn3-G), cyanidin-3-(6″-malonylglucoside) [cy3-(6-mal-G)], pelargonidin-3-(6″-malonylglucoside) [pg3-(6-mal-G)], cyanidin-3-(dimalonylglucoside) [cy3-(dimal-G)], cyanidin 3-*O*-(6″-acetylglucoside) [cy3-(6-acet-G)] and peonidin-3-(6″-malonylglucoside) [pn3-(6-mal-G)] by using liquid chromatography–ESI–mass spectrometry (Table 1). The MS/MS spectra of anthocyanins provided clear and characteristic fragmentation data. The aglycones of anthocyanins were cyanidin [molecular weight (MW; 287)], peonidin (MW; 301) and pelargonidin (MW; 271).

To determine which anthocyanins were effective in dampening mesangial hyperplasia and matrix accumulation, individual anthocyanins were tested with HG-exposed HRMC. As shown in Fig. 2B and C, inhibitory efficacies of mesangial cell proliferation and collagen IV secretion by individual anthocyanins were observed in the order of cy3-G, pn3-G, cy3-(6-mal-G), pn3-(6-mal-G)>pg3-G. Since the yields of three anthocyanins of pg3-(6-mal-G), cy3-(dimal-G) and cy3-(6-acet-G) were so minimal, the current study did not test examine their inhibitory efficacies (Fig. 3).

3.3. PCA restoration of MMP dysfunction initiated by HG

Expression of MT-1 MMP and TIMP-2 in HG-treated HRMC was examined by using Western blot analysis. It was found that HG

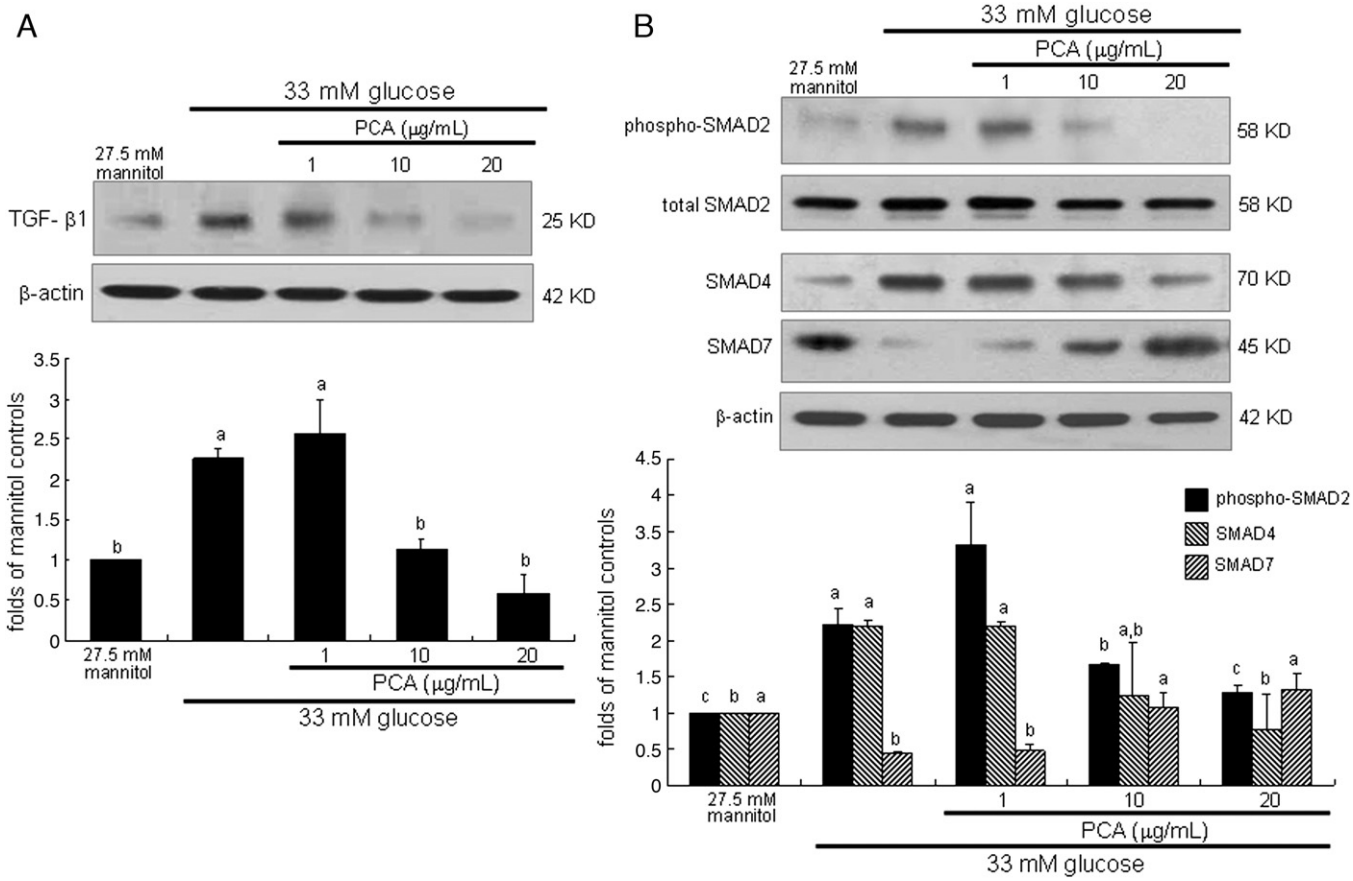

Fig. 5. Suppression of TGF-b induction (A) and SMAD signaling (B) by PCA in HG-exposed HRMCs. Cells were challenged with 1–20 μg/ml PCA and then exposed to 33 mM glucose for 3 days. HRMCs were also incubated for 3 days in 5.5 mM glucose and 27.5 mM mannitol as osmotic controls. Cell lysates were undergone to Western blot analysis with a primary antibody against TGF-β, SMAD2, phospho-SMAD2, SMAD4, SMAD7 and β-actin as an internal control. The bar graphs (mean±S.E.M., n=3) in the bottom panel represent quantitative results obtained from a densitometer. Values not sharing a letter are significantly different at P<.05.

suppressed MT1-MMP expression of HRMC and up-regulated TIMP-2 expression level (Fig. 4A). In addition, HG-exposed HRMC decreased active form of MMP-2. On the contrary, PCA boosted MT1-MMP expression and abolished TIMP-2 levels in HRMC exposed to HG.

MT-1 MMP is known to activate proMMP-2 to its active form, facilitating degradation of ECM [25]. The ECM-degrading activity of MMP-2 was examined by using gelatin zymography assay. HG suppressed conversion of proMMP-2 to its active form (Fig. 4B). However, PCA substantially enhanced gelatinolytic MMP-2 activity diminished by HG.

3.4. Disturbance of HG-activated TGF-β–SMAD signaling by PCA

TGF-β has been described to contribute a critical role in causing glomerulosclerosis and renal fibrosis [9,10]. It was tested in this study that PCA blocked HG-stimulated TGF-β signaling. When HG was solely applied to HRMC, cellular expression of TGF-β1 was enhanced (Fig. 5A). In contrast, ≥10 μg/ml PCA lessened HG-augmented cellular levels of TGF-β1.

TGF-β is known to activate the receptor-regulated SMAD2, allowing phosphorylated SMAD2 and SMAD4 complex to translocate into the nucleus for fibrogenic protein expression. Western blotting showed that HG activated SMAD2 and promoted SMAD4 expression concurrently accompanying expression blockade of inhibitory SMAD7 (Fig. 5B). When HRMCs were treated with 1–20 μg/ml PCA and exposed to HG, SMAD2 phosphorylation and SMAD4 expression were restrained in a dose-dependent manner. On the contrary, the inhibition of SMAD7 expression by HG was reversed by PCA treatments. Accordingly, PCA dampened the HG induction of TGF-β and subsequent activation of the downstream SMAD family.

3.5. Attenuation of inflammatory ICAM-1 and MCP-1 by PCA in HG-stimulated HRMC

This study elucidated that PCA may alleviate mesangial inflammation possibly involved in renal fibrotic process. HG

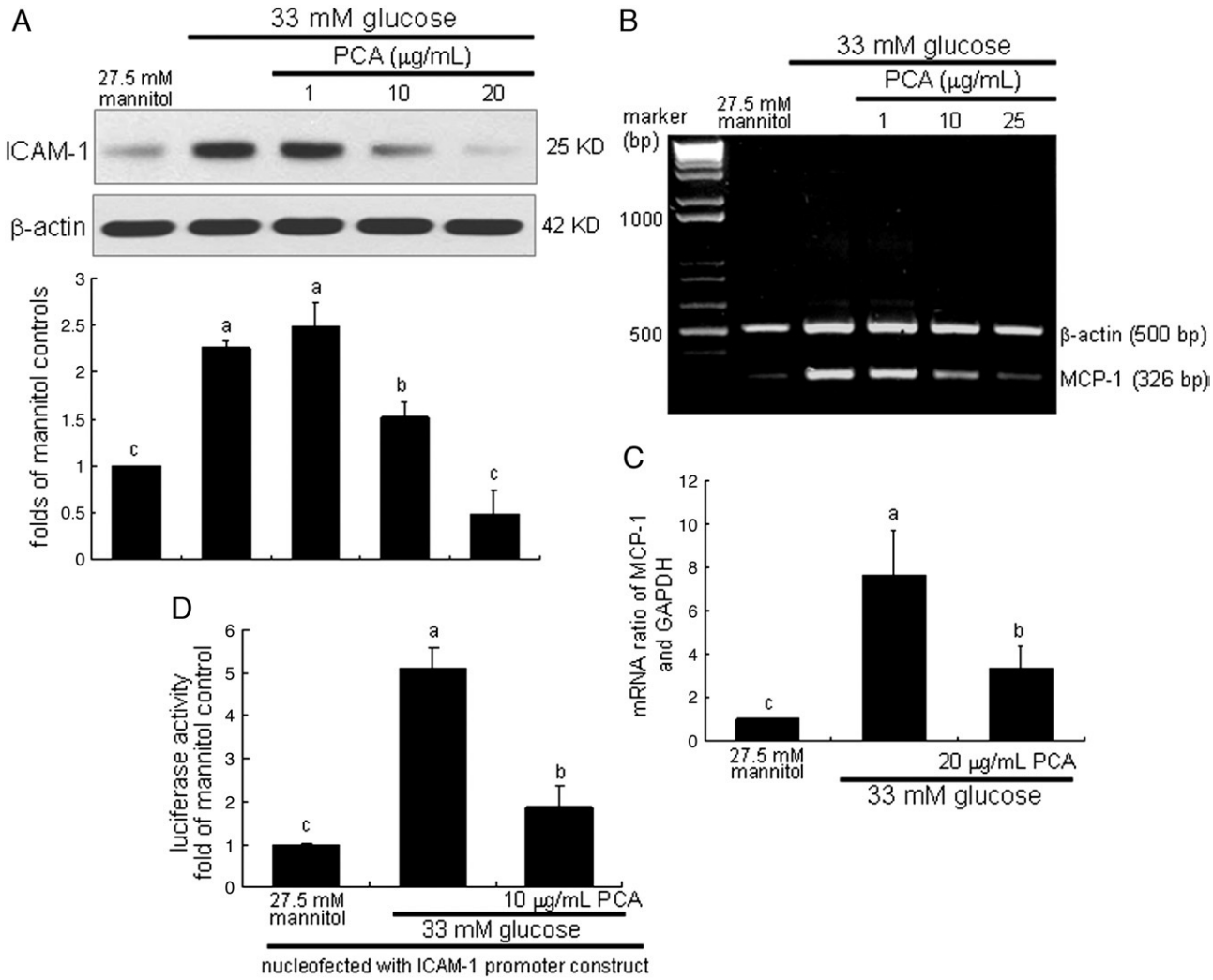

Fig. 6. Inhibition of induction of inflammatory ICAM-1 protein (A) and MCP-1 mRNA (B and C), and suppression of promoter activity of ICAM-1 (D) by PCA in HRMCs under high three D-glucose conditions. In addition, HRMCs were incubated with 5.5 mM glucose and 27.5 mM mannitol as osmotic controls. Cell lysates were used for Western blot analysis with a primary antibody against ICAM-1. β-Actin protein was used as an internal control. The bar graph (mean±S.E.M., $n=3$) in the bottom panel represents densitometric results. RT-PCR (B) and real-time PCR (C) showing mRNA levels of MCP-1 in PCA-treated and 33 mM glucose-stimulated HRMC. β-Actin genes were used as an internal control for the coamplification with MCP-1 (three separate experiments). HRMCs were nucleofected with a luciferase-harboring ICAM-1 promoter construct (D). Transfected mesangial cells (HRMC) were incubated with 33 mM glucose for 3 days in the presence of 10 μg/mL PCA. Transfected cells were incubated with 5.5 mM glucose and 27.5 mM mannitol as osmotic controls. Promoter activity was assessed using luciferase reporter gene assay. The bar graphs (means± S.E.M., $n=3$) represent quantitative results obtained from a luminometer. Values not sharing a letter are significantly different at $P<.05$.

enhanced ICAM-1 expression, which was reversed by ≥10 μg/ml PCA (Fig. 6A). In addition, MCP-1 mRNA transcript level was enhanced in HG-exposed mesangial cells, evidenced by RP-PCR and real-time PCR (Fig. 6B, C). Such enhancement was near-completely obliterated by PCA. Reporter gene luciferase activity assay showed that the promoter activity of ICAM-1, a target gene of inflammatory signaling, was markedly enhanced in mesangial cells exposed to HG (Fig. 6D). This elevation was markedly attenuated by treating transfected HRMC with 10 μg/ml PCA. This implied that ICAM-1 was an important factor responsible for HG-induced mesangial inflammation.

To test whether mesangial inflammation is involved in renal fibrosis, the role of MCP-1 in the CTGF induction was elucidated. MCP-1 stimulated CTGF expression, denoting that mesangial fibrosis was linked to MCP signaling (Fig. 7A). Interestingly, MCP-1-triggered CTGF induction was repealed by 10 μg/ml PCA. Furthermore, the ICAM-1 expression was mediated directly through TGF-β signaling as with HG, which was also repressed in PCA-treated HRMC (Fig. 7B). MCP-1 transcription was prompted in a similar fashion to ICAM-1 expression (Fig. 7C). This implies that TGF-β was an upstream regulator of proinflammatory ICAM-1 and MCP-1. It seems to be plausible that there was a crosstalk between mesangial fibrosis and inflammation that was disrupted by PCA.

3.6. Blockade of NF-κB signaling by PCA

Immunocytochemical photoimages revealed that HG triggered nuclear translocation of NF-κB of mesangial cells (Fig. 8A). The NF-κB transactivation was retarded by PCA in a dose-dependent fashion. Consistent with immunocytochemical data, there was an increase in nuclear NF-κB p65 level observed in HG-exposed HRMC, showing that

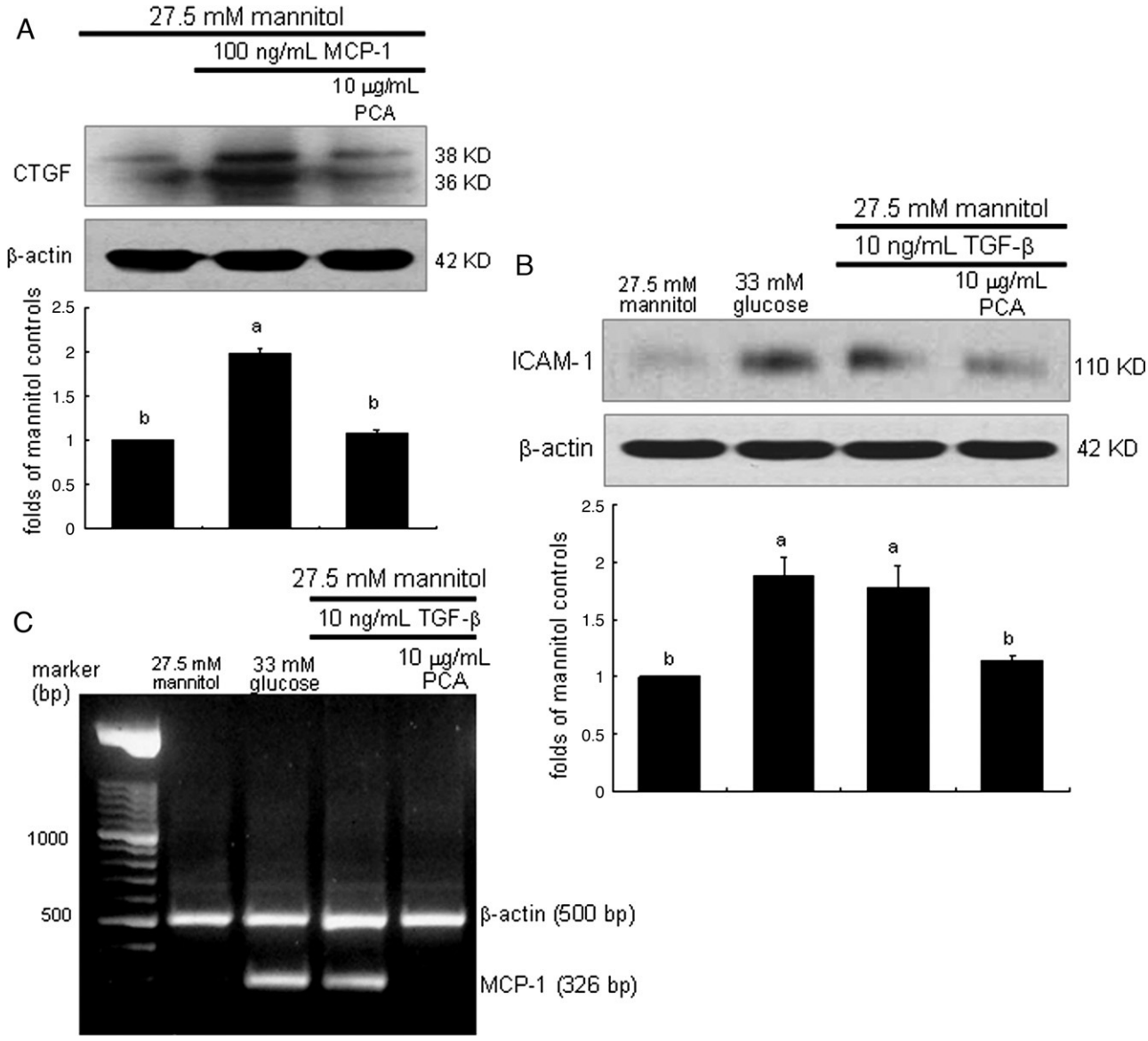

Fig. 7. Effects of PCA on CTGF induction by MCP-1 (A) and induction of ICAM-1 (B) and MCP-1 (C) by TGF-β. HRMCs were treated for 3 days with 100 ng/ml human recombinant MCP-1 or with 10 ng/ml human recombinant TGF-β in the absence and presence of 10 μg/ml PCA. Also, HRMCs were incubated with 5.5 mM glucose and 27.5 mM mannitol as osmotic controls. Cell extracts were used for Western blot analysis with a primary antibody against CTGF (A) and ICAM-1 (B). β-Actin protein was used as an internal control. The bar graphs (mean±S.E.M., $n=3$) in the bottom panels represent densitometric results, and respective blot data were obtained from three separate experiments. RT-PCR (C) showing mRNA levels of MCP-1 in 100 ng/ml TGF-β-treated and 33 mM glucose-inflamed HRMC. β-Actin genes were used as an internal control for the coamplification with MCP-1 (three separate experiments).

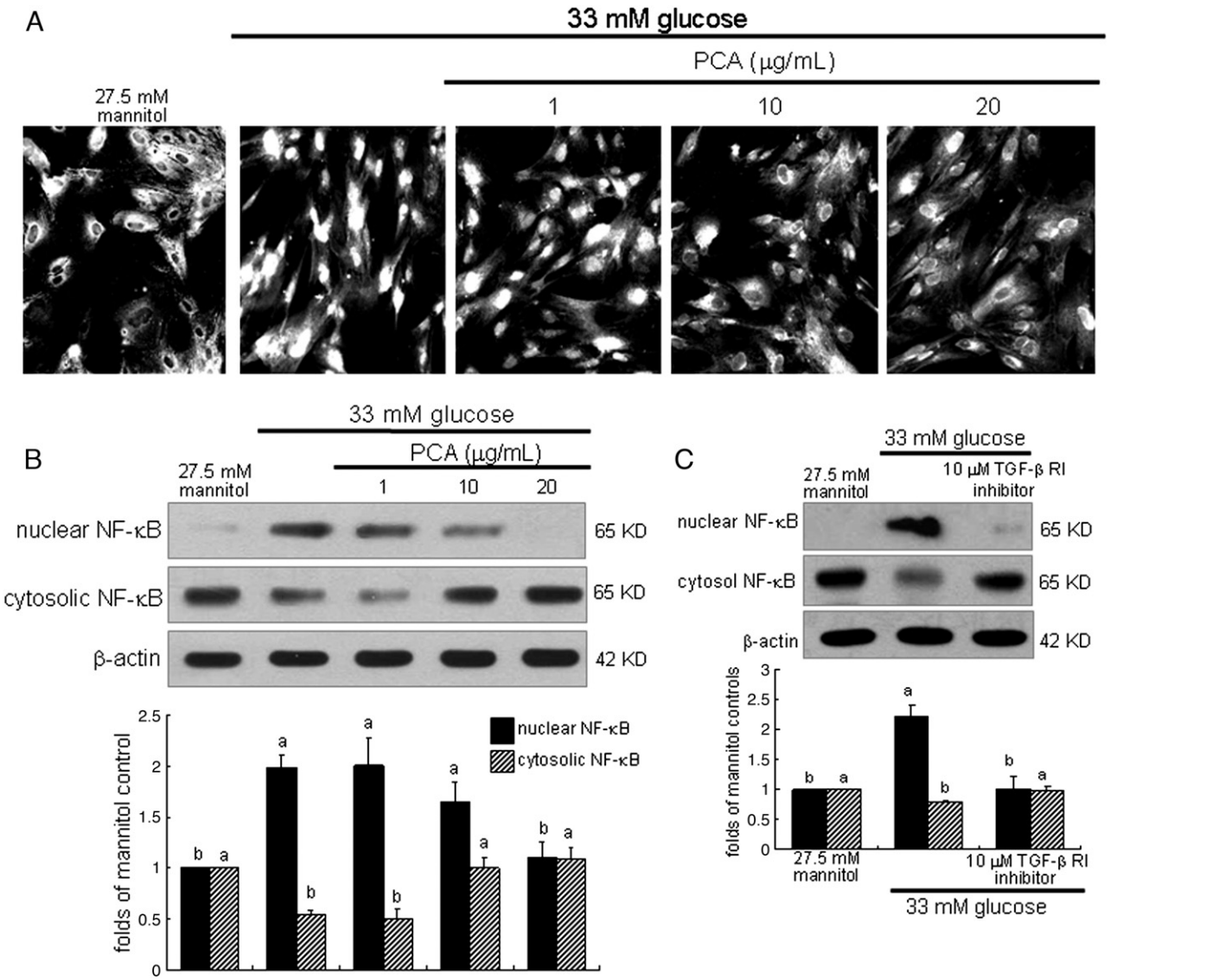

Fig. 8. Blockade of nuclear translocation of NF-kB in HRMCs treated with PCA under HG conditions (A and B) or in HRMC treated with 10 μM TGF-βR1 inhibitor (C). Confluent HRMCs were incubated with 1–20 μg/mL PCA for 3 days under the conditions of HG. HRMCs were also incubated with 5.5 mM glucose and 27.5 mM mannitol as osmotic controls. Immunocytochemistry (A) was conducted to visualize nuclear translocation of NF-κB. Antibody localization was detected with fluorescein isothiocyanate-conjugated antirabbit IgG. Magnification: 200-fold. For Western blot analysis with a primary antibody against NF-κB (B and C), cytosolic and nuclear fractions were obtained. β-Actin protein was used as an internal control. Respective blot data were obtained from three independent experiments. The bar graphs (mean±S.E.M., $n=3$) in the right panel represent densitometric results, and values not sharing a letter are significantly different at $P<.05$.

HG enhanced nuclear translocation of NF-κB (Fig. 8B). As expected, PCA at 10 μg/ml blunted nuclear translocation of NF-κB.

This study attempted to elucidate that NF-κB signaling was involved in the crosstalk between mesangial fibrosis and inflammation. Nuclear translocation of NF-κB stimulated by HG was abolished in the presence of a TGF-β receptor kinase 1 (TGF-βR1) inhibitor, which indicates that TGF-β-induced mesangial fibrosis is most likely mediated by NF-κB signaling (Fig. 8C). Furthermore, the induction of CTGF, ICAM-1 and MCP-1 was determined in HG-exposed HRMC in the presence of the NF-κB inhibitor SN50. The CTGF expression elevated in HG-exposed mesangial cells was mitigated by the presence of 10 μM SN50 (Fig. 9A). In addition, the induction of ICAM-1 protein and MCP-1 transcript by HG was demoted in SN50-experienced HRMC (Fig. 9B, C). Accordingly, NF-κB signaling was possibly involved in the crosslink between diabetes-associated mesangial fibrosis and inflammation.

4. Discussion

Anthocyanins, which are used as a food coloring, are widely distributed in human diets, suggesting that we ingest large amounts of anthocyanins from plant-based foods. Anthocyanins are a class of flavonoids with high antioxidant ability, which is responsible for bright colors visible in most fruits and vegetables [22]. Interest in anthocyanins as natural colorants and value-added ingredients has increased due to their color characteristics and potential health benefits. Purple corn has been used for centuries as natural food colorants and drinks in South America. Chinese purple corn extracts (*Z. mays* L.) were a natural source of anthocyanins and were stable over a wide range of temperatures and times [26]. This study found eight disparate monomeric anthocyanins with high variability of contents in purple corn extracts. Inhibitory efficacies of mesangial hyperplasia and matrix

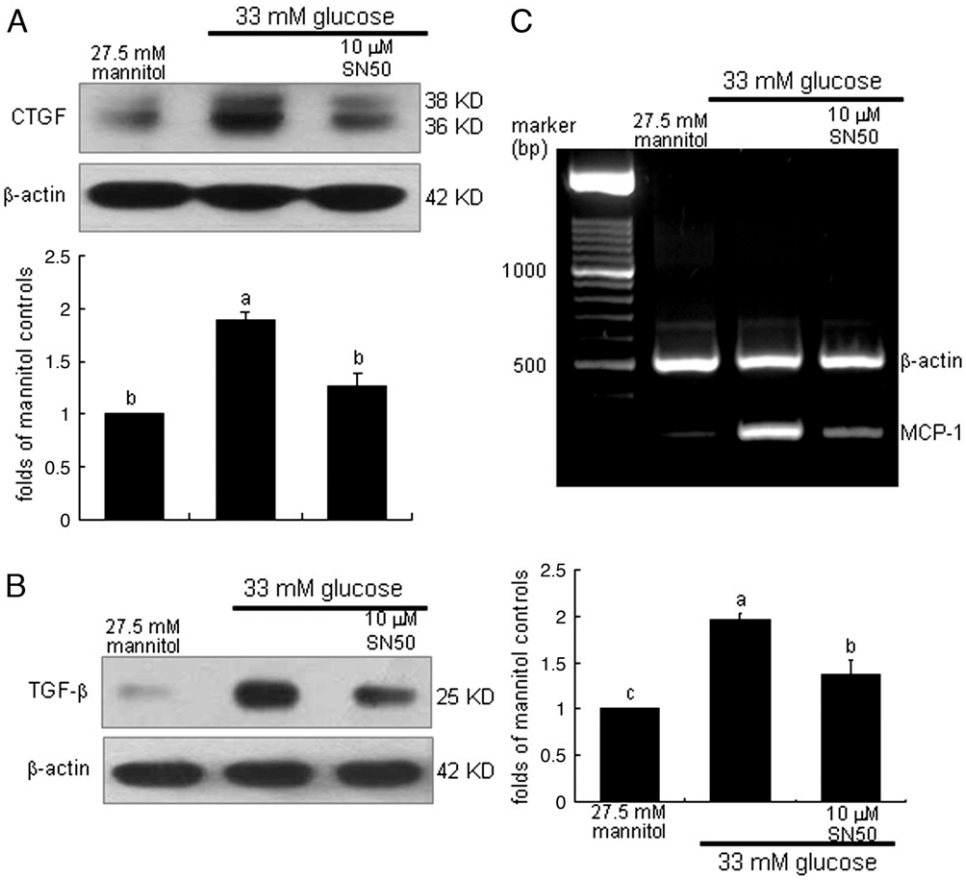

Fig. 9. Inhibition of CTGF (A), TGF-β (B) and MCP-1 (C) in NF-κB inhibitor SN50-treated HRMCs. HRMCs were incubated with 33 mM glucose for 3 days in the presence of 10 μM SN50 or 5.5 mM glucose plus 27.5 mM mannitol as osmotic controls. For protein expression of CTGF and TGF-β (A and B), Western blot analysis was conducted using a primary antibody against CTGF and TGF-β. β-Actin protein was used as an internal control. The bar graphs (mean±S.E.M., $n=3$) in the bottom panel represent quantitative results obtained from a densitometer. Values not sharing a letter are significantly different at $P<.05$. RT-PCR (C) showing the steady-state mRNA transcriptional levels of MCP-1 in 10 μM SN50-treated and 33 mM glucose-stimulated HRMC. β-Actin genes were used as an internal control for the coamplification with MCP-1 (three separate experiments).

accumulation by the major anthocyanins among eight disparate anthocyanins were observed in the order of cy3-G, pn3-G, cy3-(6-mal-G), pn3-(6-mal-G)>pg3-G.

Various phenolic fractions obtained from Andean purple corn exhibited antimutagenic and antioxidant properties [27]. This study evaluated whether anthocyanins rich in purple corn color retarded chronic hyperglycemia-induced mesangial hyperplasia and renal fibrosis. Purple corn extract rich in anthocyanins suppressed proliferation of human colorectal adenocarcinoma HT29 cells and exerted an additive interaction with the other functional phenolics [17,22]. Anthocyanins showed antiangiogenic, antidiabetic and anticarcinogenic properties for potential medicinal uses [18–20]. Cyanidin 3-glucoside, a major anthocyanin present in purple corn color, suppressed 7,12-dimethylbenz[*a*]anthracene-induced mammary carcinogenesis, indicating that purple corn color may be a promising chemotherapeutic agent [21]. In addition, cy3-G-rich purple corn color or anthocyanins ameliorated insulin resistance and suppressed the mRNA levels of enzymes involved in fatty acid and triacylglycerol synthesis and lowered the sterol regulatory element binding protein-1 mRNA level in white adipose tissue in mice, indicating that may have benefits for the prevention of obesity and diabetes [28].

DN is characterized by aberrant alterations in ECM ultimately leading to chronic renal failure [1]. The first and most distinctive glomerular lesion of diabetes is mesangial expansion concurrently accompanying mesangial hyperplasia, which precedes diabetic glomerulosclerosis [2,3]. A boosted production of matrix-synthesizing growth factors and a diminished formation of matrix-degrading proteases contribute to hyperglycemia-associated accumulation of ECM constituents at the glomerular levels [4,5]. CTGF are expressed in the mesangium and play an important role in the ECM-synthesizing process, while MMP is involved in inducing the enzymatic breakdown of ECM [1,4]. In addition, hyperglycemia stimulated induction of fibrogenic and prosclerotic cytokines activating ECM deposition through instigating intracellular signalings [3,8]. Increased TGF-β is considered as a major fibrogenic cytokine involved in the progression of DN 0. High ambient glucose stimulated resident renal cells to produce TGF-β1, possibly enhancing ECM accumulation [9,10]. In this study, there were eight major anthocyanins identified in the kernel of purple corn that exhibited disparate effects on the inhibition of HG-promoted cell proliferation and collagen IV secretion. In addition, PCA dampened mesangial hyperplasia and CTGF-linked ECM accumulation in chronic diabetic condition.

The current study attempted to elucidate how PCA prevented mesangial ECM accumulation in HG-exposed mesangial cell models. PCA improved the HG-triggered MMP system dysfunction by enhancing ECM-degrading MT-1 MMP expression and repealing TIMP-2 expression. Accordingly, compelling evidence was drawn from this study that PCA had the potential capability to block HG-induced glomerulosclerosis and renal fibrosis. Similarly, *Ginkgo biloba* extract postponed the ECM accumulation by promoting the degradation of ECM through the activation of the MMP system in rat mesangial cells [29]. Furthermore, TGF-β was identified as a

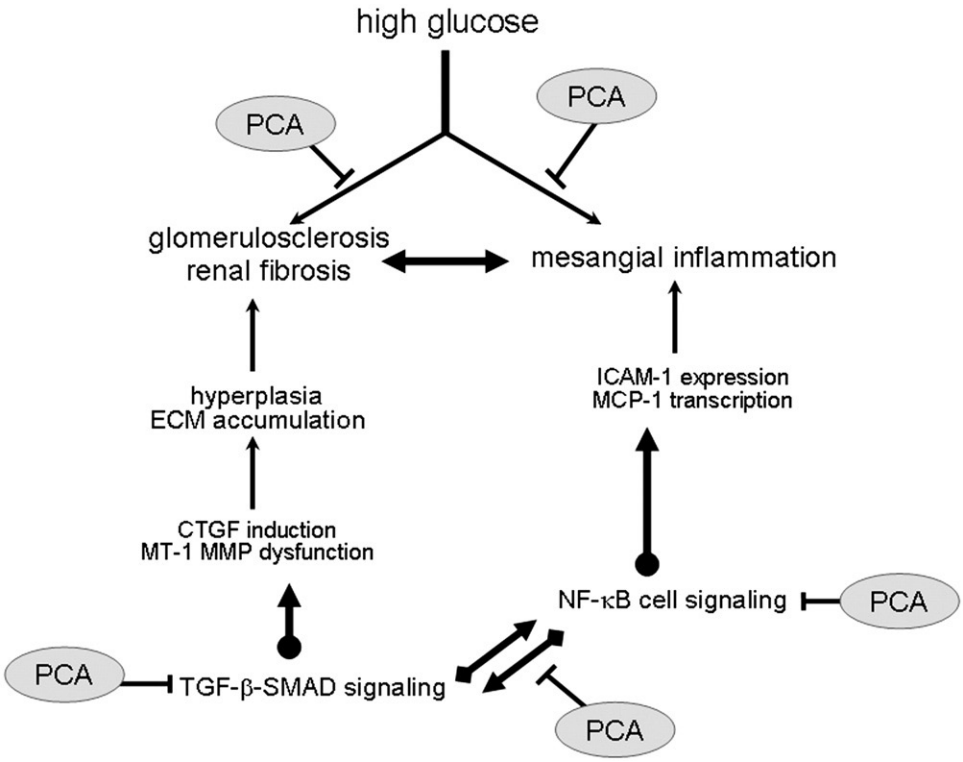

Fig. 10. Schematic diagram showing actions of PCA disturbing crosstalk between mesangial fibrosis and inflammation pathways entailing TGF-β and NF-κB. The symbol indicates stimulation (→) due to HG or blockade (⊥) due to supplementation of PCA.

critical factor in renal diseases by stimulating mesangial cell proliferation and ECM production and inducing epithelial–mesenchymal transformation in renal tissue [9]. TGF-β–SMAD signaling has been reported to play a vital role in the process of ECM expansion [8–10]. SMAD3 and SMAD4 but not SMAD2 were required for TGF-β1-induced CTGF promoter activity and expression in osteoblasts [30]. In this study, PCA disturbed the TGF-β-SMAD signal pathway through retarding TGF-β expression and downstream activation of SMAD2 and SMAD4 and enhancing the level of inhibitory SMAD7.

There is accumulating evidence demonstrating that the diabetes-associated nephropathy is closely related to mesangial inflammation [11,12]. In diabetic patients with nephropathy, the levels of ICAM-1 and MCP-1 recruiting inflammatory immune cells of macrophages and granulocytes were elevated [11,12,31]. It was shown that MCP-1 appeared to be responsible for diabetic ECM accumulation and early inflammation in DN pathogenesis [13]. In this study, MCP-1 was involved in mediating the CTGF induction by TGF-β leading to ECM deposition. In addition, like HG, TGF-β per se induced ICAM-1 and MCP-1, which was deregulated by PCA. Natural compounds have been reported as potential agents alleviating renal stress-triggered inflammation [14,15]. Isoflavone puerarin suppressed mesangial inflammation induced by advanced glycation end-product likely through the induction of heme oxygenase-1 expression [15]. In addition, colchicine dampened inflammatory cell infiltration and ECM accumulation in DN, which was mediated by MCP-1 and ICAM-1 blockade [16]. Therefore, these natural compounds may retard mesangial inflammation and ECM accumulation via disturbing inflammatory and fibrogenic pathways. However, the crosstalk between mesangial fibrosis and inflammation has not yet been well defined.

This study was to evaluate the nutritional and pharmacological effects of PCA on diabetes-associated mesangial inflammation in human mesangium by elucidating crosstalk between mesangial fibrosis and inflammation. Much is known about the bioactive properties of anthocyanins, but very little work has been done to determine the properties of anthocyanins in renal fibrosis and glomerular sclerosis. This study revealed that PCA blunted nuclear translocation of NF-κB, suggesting that its signaling was involved in the crosstalk between mesangial fibrosis and inflammation. In deed, the induction of ICAM-1 protein and MCP-1 transcript was demoted in mesangial cells exposed to HG and experienced with a NF-κB inhibitor. The polyphenol resveratrol was a strong antifibrogenic agent in the CCl_4 model of cirrhosis, which was probably associated with the ability of resveratrol to reduce NF-κB activation and TGF-β content [32].

In summary, this study revealed that PCA retarded diabetes-associated renal fibrosis and mesangial inflammation through disturbing TGF-β signaling (Fig. 10). PCA dampened HG-inflamed hyperplasia and CTGF-induced ECM expansion by improving matrix-degrading MMP system involving TIMP-2. The HG-stimulated CTGF induction entailed TGF-β-SMAD-responsive pathways that were encumbered by PCA. In addition, PCA attenuated TGF-β-triggered inflammatory ICAM-1 expression and MCP-1 production in the mesangium. The capability of PCA to deter renal fibrosis and mesangial inflammation may be promising in hampering the progression of renal fibrosis to end-stage renal diseases. Furthermore, diabetes-associated renal fibrosis was most likely linked to mesangial inflammation, which was mediated by a crosstalk between TGF-β and NF-κB signaling disrupted by PCA. Therefore, the renoprotection of PCA against mesangial inflammation may be specific therapies of renal fibrosis in DN.

References

[1] Ban CR, Twigg SM. Fibrosis in diabetes complications: pathogenic mechanisms and circulating and urinary markers. Vasc Health Risk Manag 2008;4:575–96.

[2] Schena FP, Gesualdo L. Pathogenetic mechanisms of diabetic nephropathy. J Am Soc Nephrol 2005;16:S30–3.
[3] Kanwar YS, Wada J, Sun L, Xie P, Wallner EI, Chen S, et al. Diabetic nephropathy: mechanisms of renal disease progression. Exp Biol Med (Maywood) 2008;233: 4–11.
[4] Pozzi A, Voziyan PA, Hudson BG, Zent R. Regulation of matrix synthesis, remodeling and accumulation in glomerulosclerosis. Curr Pharm Des 2009;15: 1318–33.
[5] Thrailkill KM, Clay Bunn R, Fowlkes JL. Matrix metalloproteinases: their potential role in the pathogenesis of diabetic nephropathy. Endocrine 2009; 35:1–10.
[6] Riser BL, Cortes P. Connective tissue growth factor and its regulation: a new element in diabetic glomerulosclerosis. Ren Fail 2001;23:459–70.
[7] McLennan SV, Martell SK, Yue DK. Effects of mesangium glycation on matrix metalloproteinase activities: possible role in diabetic nephropathy. Diabetes 2002;51:2612–8.
[8] Pohlers D, Brenmoehl J, Löffler I, Müller CK, Leipner C, Schultze-Mosgau S, et al. TGF-β and fibrosis in different organs — molecular pathway imprints. Biochim Biophys Acta 2009;1792:746–56.
[9] Fukuda N, Tahira Y, Matsuda H, Matsumoto K. Transforming growth factor-β as a treatment target in renal diseases. J Nephrol 2009;22:708–15.
[10] Giannico G, Cortes P, Baccora MH, Hassett C, Taube DW, Yee J. Glibenclamide prevents increased extracellular matrix formation induced by high glucose concentration in mesangial cells. Am J Physiol Renal Physiol 2007;292: F57–65.
[11] Fornoni A, Ijaz A, Tejada T, Lenz O. Role of inflammation in diabetic nephropathy. Curr Diabetes Rev 2008;4:10–7.
[12] Chen L, Zhang J, Zhang Y, Wang Y, Wang B. Improvement of inflammatory responses associated with NF-κB pathway in kidneys from diabetic rats. Inflamm Res 2008;57:199–204.
[13] Chao CY, Mong MC, Chan KC, Yin MC. Anti-glycative and anti-inflammatory effects of caffeic acid and ellagic acid in kidney of diabetic mice. Mol Nutr Food Res 2010;54:388–95.
[14] Lee HT, Kim M, Kim M, Kim N, Billings IV FT, D'Agati VD, et al. Isoflurane protects against renal ischemia and reperfusion injury and modulates leukocyte infiltration in mice. Am J Physiol Renal Physiol 2007;293:F713–22.
[15] Jung KJ, Go EK, Kim JY, Yu BP, Chung HY. Suppression of age-related renal changes in NF-κB and its target gene expression by dietary ferulate. J Nutr Biochem 2009;20:378–88.
[16] Li JJ, Lee SH, Kim DK, Jin R, Jung DS, Kwak SJ, et al. Colchicine attenuates inflammatory cell infiltration and extracellular matrix accumulation in diabetic nephropathy. Am J Physiol Renal Physiol 2009;297:F200–9.
[17] Jing P, Giusti MM. Effects of extraction conditions on improving the yield and quality of an anthocyanin-rich purple corn (*Zea mays* L.) color extract. Food Chem Toxicol 2007;72:366–8.
[18] Wang LS, Stoner GD. Anthocyanins and their role in cancer prevention. Cancer Lett 2008;269:281–90.
[19] Zafra-Stone S, Yasmin T, Bagchi M, Chatterjee A, Vinson JA, Bagchi D. Berry anthocyanins as novel antioxidants in human health and disease prevention. Mol Nutr Food Res 2007;51:675–83.
[20] Crozier A, Jaganath IB, Clifford MN. Dietary phenolics: chemistry, bioavailability and effects on health. Nat Prod Rep 2009;26:1001–43.
[21] Fukamachi K, Imada T, Ohshima Y, Xu J, Tsuda H. Purple corn color suppresses Ras protein level and inhibits 7,12-dimethylbenz[*a*]anthracene-induced mammary carcinogenesis in the rat. Cancer Sci 2008;99:1841–6.
[22] Jing P, Bomser JA, Schwartz SJ, He J, Magnuson BA, Giusti MM. Structure-function relationships of anthocyanins from various anthocyanin-rich extracts on the inhibition of colon cancer cell growth. J Agric Food Chem 2008;56: 9391–8.
[23] Kang SW, Choi JS, Bae JY, Li J, Kim DS, Kim JL, et al. Blockade of vascular angiogenesis by *Aspergillus usamii* var. shirousamii-transformed *Angelicae gigantis* Radix and *Zizyphus jujuba*. Nutr Res Pract 2009;3:3–8.
[24] Li J, Lee YS, Choi JS, Sung HY, Kim JK, Lim SS, et al. Roasted licorice extracts dampen high glucose-induced mesangial hyperplasia and matrix deposition through blocking Akt activation and TGF-β signaling. Phytomedicine 2010;17: 800–10.
[25] Kang SW, Choi JS, Choi YJ, Bae JY, Li J, Kim DS, et al. Licorice isoliquiritigenin dampens angiogenic activity via inhibition of MAPK-responsive signaling pathways leading to induction of matrix metalloproteinases. J Nutr Biochem 2010;21: 55–65.
[26] Zhao X, Corrales M, Zhang C. Composition and thermal stability of anthocyanins from chinese purple corn (*Zea mays* L.). J Agric Food Chem 2008;56:10761–6.
[27] Pedreschi R, Cisneros-Zevallos L. Antimutagenic and antioxidant properties of phenolic fractions from Andean purple corn (*Zea mays* L.). J Agric Food Chem 2006;54:4557–67.
[28] Tsuda T, Horio F, Uchida K, Aoki H, Osawa T. Dietary cyanidin 3-*O*-β-D-glucoside-rich purple corn color prevents obesity and ameliorates hyperglycemia in mice. J Nutr 2003;133:2125–30.
[29] Ji L, Yin XX, Wu ZM, Wang JY, Lu Q, Gao YY. *Ginkgo biloba* extract prevents glucose-induced accumulation of ECM in rat mesangial cells. Phytother Res 2009;23:477–85.
[30] Arnott JA, Zhang X, Sanjay A, Owen TA, Smock SL, Rehman S, et al. Molecular requirements for induction of CTGF expression by TGF-β1 in primary osteoblasts. Bone 2008;42:871–85.
[31] Min D, Lyons JG, Bonner J, Twigg SM, Yue DK, McLennan SV. Mesangial cell-derived factors alter monocyte activation and function through inflammatory pathways: possible pathogenic role in diabetic nephropathy. Am J Physiol Renal Physiol 2009;297:F1229–1237.
[32] Chávez E, Reyes-Gordillo K, Segovia J, Shibayama M, Tsutsumi V, Vergara P, et al. Resveratrol prevents fibrosis, NF-κB activation and TGF-β increases induced by chronic CCl_4 treatment in rats. J Appl Toxicol 2008;28:35–43.